OPTIMAL VIBRATION CONTROL OF A MILLING ELECTROSPINDLE

Vincent Tamisier[♦], Stéphane Font[⊠]

[♦] ESTACA, Control & Systems Laboratory, 34 rue Victor Hugo, 92300 Levallois Perret, France

[⊠] Supélec, Service Automatique, Plateau de Moulon, 91192 Gif sur Yvette, France

vtamisier@estaca.fr

ABSTRACT

We present the case study of a five-axis high speed milling electro-spindle on AMBs. A Finite Element Model is developed in order to obtain a state-space model of the flexible shaft. This model is supplemented by a second state-space model, representing the rigid behaviour induced by the closed loop composed of the active magnetic bearings, actuators, sensors and the controller.

An active unbalance control algorithm has been developed, based on the considerations of [1]. This method gives an absolute control on the unbalance vibrations. We obtain excellent results, as we expected. But we also aim at milling steel, at a rotational speed close to the rigid modes, and yet this method reduces the stiffness of the bearings at the rotational speed.

For stability reasons, we then needed another method that could compensate perfectly the unbalance without adding any closed-loop to the systems. For this open-loop method, a statistical study, considering the variance of the estimator and various extra signals give good insight on the result. We finally present some practical results based on milling experiments.

INTRODUCTION

The machine is a five-axis high speed milling electro-spindle on AMBs, equipped with a permanent magnet motor. Its maximal power is 40 kW at 40000 rpm.

Complex rotors are usually modelled by means of Finite Element Method (FEM) to cope with non-elementary shape of the shaft and of the rotating appendices connected to it. A possible output of a FEM software is the frequency response (Bode diagram) of the shaft, which most of the time is enough for the enlarged PID controller design. But this is not enough for time simulations of advanced control algorithms. That's why we had to extract from the frequency response a transfer function numerical model. We used the singular value decomposition method for a frequency domain Identification. In order to minimise the order of the identified model, a pole-zero cancellation method can be used afterwards, but whatever the result may be, the order remains higher than the real one if we want to preserve the accuracy for time domain simulations.

The system seemed to show few gyroscopic effects (responsible for the modes splitting); the decision was then taken to consider the frequency responses at the nominal speed only. The tool was also modelled and taken into account in the estimation. We illustrate the comparison between the reduced-order estimated transfer function and the original frequency response, for the four terms of the matrix-form model. It can be observed that a better accuracy is achieved on the modes than on the central zeros.

The aim is to identify the unbalance in order to minimize the command, responsible for the vibrations, before crossing the rigid mode or around its value. For stability reasons, the well-known unbalance control algorithm ABS can only operate when the rotational speed is about 20% greater than the frequency of the rigid mode, which value is imposed at 150 Hz by the means of the controller. Yet, the objective is to use the spindle for milling steel, precisely at a speed close to this frequency. That's why a new method that preserve the stability of the system had to be designed.

An improved unbalance control algorithm based on [1] has been developed in order to minimise the vibrations for an optimal operation of the spindle. For stability reasons, we then needed another method that could compensate perfectly the unbalance without adding any closed-loop to the systems, because the first method reduced the stiffness at the rotational

speed. It's a four-step method that consists in identifying both the unbalance and the synchronous sensitivity function with two measurements, thanks to two different synchronous signals added. For this open-loop method, a statistical study, considering the variance of the estimator and various extra signals give good insight on the result. We finally present some practical results based on milling experiments.

DESCRIPTION OF THE MILLING SPINDLE

The high speed milling machine considered is a machine tool spindle equipped with a permanent magnet motor (see Figure 1). It uses a five-axis AMB technology.

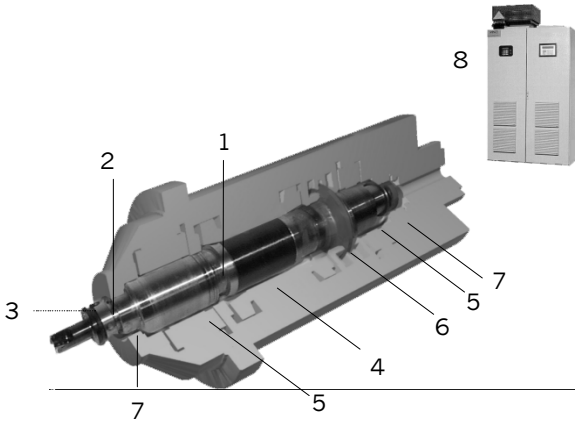

FIGURE 1: design of the milling machine

The milling machine design: (1) 80 mm diameter shaft, (2) HSK tool attachment, (3) OTT tool changer, (4) permanent magnet motor, (5) radial bearings on each side of the motor, (6) large thrust bearing disc at the rear part, (7) two auxiliary bearing sets for additional safety, (8) motor drive inverter and magnetic bearing control system cabinet.

The DC brushless, permanent magnet motor (4) design is unique. Powerful samarium-cobalt magnets are aligned along the shaft axis and contained by a carbon-fibre sleeve. This design has been tested and operated for 6 years. The main feature is the fact that this type of motor is synchronous. Synchronous motors offer much lower losses and better control accuracy over asynchronous motors. The main characteristics of the milling spindle are indicated on table 1.

Speed	0-40000 rpm
Max speed	45000 rpm
Nominal power	33 kW at 40000 rpm
Max power	40 kW at 40000 rpm
Outer Diameter	220h6
Tool attachment	HSK 50 A
ATC	OTT (DIN 69893)
Acceleration (0-V max)	7 seconds
Braking (V max-0)	7 seconds

TABLE 1: Main characteristics of the spindle

Compared with the conventional milling process, the high speed milling on AMBs provides many advantages: any tool rupture is instantaneously detected either in the form of force vibration, shaft displacement or sudden unbalance by the computer numerical control. The safety system reaction is as quick as 200 ms. Automatic stop with no manual attendance constitute this unique built-in safety design. Moreover, the surface quality of the machined parts depends on spindle shaft stiffness; the parameters of the dynamic stiffness can be controlled through numerical control.

STATE-SPACE MODEL

We use a Finite Element Method (FEM) to predict the flexible behaviour of the system. To account for the complex geometry, the discretization at the base of the FEM model is usually characterized by a high number of nodes and, correspondingly, of degrees of freedom. When AMB are concerned, a model is necessary to design the control law to stabilize the complete system represented by the shaft and the AMBs.

It is possible to extract from the frequency response a transfer function in order to have a numerical model. We use in this case a singular value decomposition method for a so-called frequency domain identification. In order to minimize the identified model, a pole-zero cancellation method can be used afterwards, but whatever the result may be, the order remains higher than the expected one. Moreover, the accuracy of estimation for the zeros is not that good, and this kind of model is a final issue, when the machine is already built and suspended, which is restrictive.

What we need is a polyvalent numerical model, not only for designing the control laws needed to stabilize the system but also for simulating anti-vibration algorithms, making time domain simulations and so on.

The first step consists in building a model for the flexible rotor that represent the state of each node. We use the method presented in [2] in order to extract the data we need for building the modal state-space model of the flexible shaft.

The typical values to define the complete geometry of the rotor are $n = 50$ nodes, and $p = 4$ degrees of freedom per node. The following set equations (1) and (2) represent the state-space form of the mechanical equation of the flexible system (see [3]).

$$\dot{\delta} = \begin{pmatrix} -M^{-1}(D+\Omega G) & -M^{-1}K \\ I & 0 \end{pmatrix}\delta + \begin{pmatrix} B \\ 0 \end{pmatrix}F \qquad (1)$$

$$Y = \begin{pmatrix} C & 0 \end{pmatrix}\delta \qquad (2)$$

M, D, G, K are respectively the mass, damping, gyroscopic and stiffness matrix. X is the vector containing the np degrees of freedom. F represents the electromagnetic forces, and B the nodes where those forces are applied. Ω is the rotational speed. δ is the state vector containing all the displacements for all the nodes.

The resulting state-space model has an order $N = 2np$ (usually $N = 400$), that makes it uneasy or even heavy to use for calculation. Moreover, such an accuracy concerning all the nodes is not necessary. We propose a modal reduction of the system. The so-called modes are the square roots of the eigenvalues of the $M^{-1}K$ matrix. Let Φ be the matrix composed of the eigenvectors associated to the m flexible modes we want to observe. A new state vector μ of size m as described in equation (4) is used.

$$X = \Phi\mu \qquad (4)$$

A matrix of eigenvectors Φ is chosen as to obtain $\Phi^T M \Phi = I$. Let χ defined by (5) be the state vector of the modal state-space model.

$$\chi = \begin{pmatrix} \dot{\mu} \\ \mu \end{pmatrix} \qquad (5)$$

With $D_M = \Phi^T(D+\Omega G)\Phi$ and $K_M = \Phi^T K \Phi$ we then obtain with (6) and (7) the expression of the state-space modal model of the shaft:

$$\dot{\chi} = \begin{pmatrix} -D_M & -K_M \\ I & 0 \end{pmatrix}\chi + \begin{pmatrix} \Phi^T B \\ 0 \end{pmatrix}F \qquad (6)$$

$$Y = \begin{pmatrix} C\Phi & 0 \end{pmatrix}\chi \qquad (7)$$

The order of this model is $2m$. Once a flexible modal model for the rotor is obtained, we need to take into account the rigid behaviour of the system. The rigid part of the system depends on its geometry, the positions of the actuators and the positions of the detectors (see [4]).

Any movement of a rigid rotor inside its AMBs can be represented as a combination of a translation movement and a tilting movement. The bearings generate the forces F_1 and F_2. The displacements of the rotor on the detectors are called x_1 and x_2, while x is the displacement of the center of gravity G. α is the angle of rotation of the rotor during a tilting movement around G. L_{b1}, L_{b2}, L_{d1}, L_{d2} are respectively the distances from G to the first and second bearings, and to the first and second detectors. Let J be the axial moment of inertia of the rotor, and M its mass.

We obtain the following state-space form in equations (8) and (9).

$$\frac{d}{dt}\begin{pmatrix} x \\ \dot{x} \\ \alpha \\ \dot{\alpha} \end{pmatrix} = \begin{pmatrix} 0 & 1 & 0 & 0 \\ 0 & 0 & 0 & 0 \\ 0 & 0 & 0 & 1 \\ 0 & 0 & 0 & 0 \end{pmatrix}\begin{pmatrix} x \\ \dot{x} \\ \alpha \\ \dot{\alpha} \end{pmatrix} + \begin{pmatrix} 0 & 0 \\ M^{-1} & M^{-1} \\ 0 & 0 \\ L_{b1}J^{-1} & L_{b2}J^{-1} \end{pmatrix}\begin{pmatrix} F_1 \\ F_2 \end{pmatrix} \qquad (8)$$

$$\begin{pmatrix} x_1 \\ x_2 \end{pmatrix} = \begin{pmatrix} 1 & 0 & L_{d1} & 0 \\ 1 & 0 & L_{d2} & 0 \end{pmatrix}\begin{pmatrix} x \\ \dot{x} \\ \alpha \\ \dot{\alpha} \end{pmatrix} \qquad (9)$$

MODEL VALIDATION AND CONTROLLER

The final model for the rotor equipped with its magnetic bearings is composed of the sum of two terms: the rigid part of the magnetically suspended body, and the expression of the flexible behaviour of the rotor.

The model we obtain for the machine is then compared to identified transfer functions. We take into account four transfer functions, corresponding to the transfers from the forces to the displacements in the V plane, as given in (10):

$$\begin{bmatrix} x_1 \\ x_2 \end{bmatrix} = \begin{bmatrix} T_{11} & T_{12} \\ T_{21} & T_{22} \end{bmatrix}\begin{bmatrix} F_1 \\ F_2 \end{bmatrix} \qquad (10)$$

The system seemed to show few gyroscopic effects; we then consider the frequency responses at the nominal speed only. The tool was also modeled and taken into account in the estimation.

The following figure 2 illustrates the comparison between the reduced-order estimated transfer function (solid) and the original frequency response (dotted), for the two crossed terms of the matrix in

equation (1): T_{12} and T_{21}. It can be observed that a better accuracy is achieved on the modes than on the central zeros.

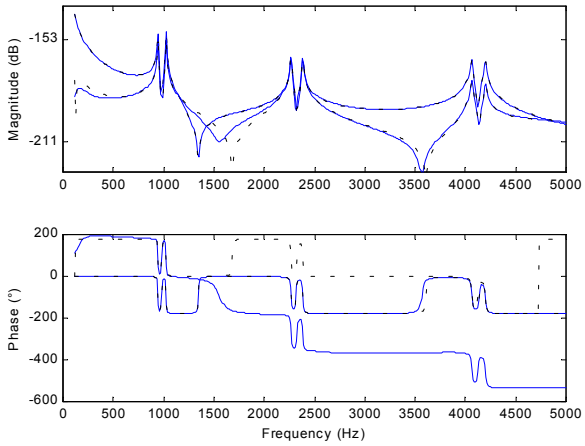

FIGURE 2: Bode diagrams of T_{12} and T_{21}

The controller is tuned considering the evolution of the modes. The robust control leads to the following sensibility function for axis 11 (figure 3).

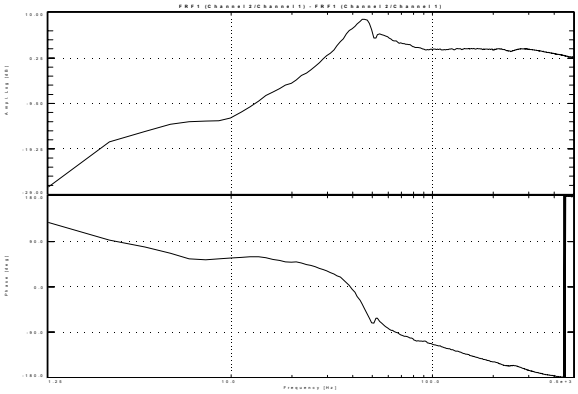

FIGURE 3: Sensibility function for axis 11

UNBALANCE CONTROL

For a rotor, the unbalance represents the difference between the axis of inertia and the geometrical axis imposed by the bearings. This gap comes from the imperfections of the rotor balancing. During the rotation, the unbalance can be observed by the means of the vibrations it induces on the system. Cancelling the unbalance effect on the system thus consists in merging the rotational axis of the bearings and the axis of inertia of the rotor.

Let m be a mass, placed at a distance d of the axis of inertia of a rotor with a rotational speed of Ω.

This mass creates a centrifugal force:

$$F = m\,d\,\Omega^2 \sin(\Omega t + \varphi) \tag{11}$$

The unbalance is the md product. If M is the mass of the rotor, this product can be reduced by defining:

$$\varepsilon = \frac{md}{M} \tag{12}$$

which is the distance between the axis of inertia and the geometric axis of the rotor.

In order to understand the unbalance compensation method, let's consider a simplified SISO model of the system, without the gyroscopic effects.

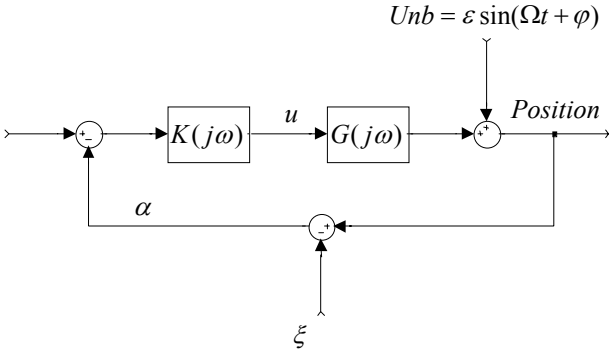

FIGURE 4: Unbalance model

$Unb = \varepsilon \sin(\Omega t + \varphi)$ represents the unbalance signal. ξ is an external input for the compensation signal, and α is the measurement used by the control. The aim is to minimize the oscillations of the control signal u and conjointly the force due to actuators, responsible for the vibrations, before crossing the rigid mode or around its value. If we choose $\xi = Unb$, the compensation is perfectly achieved and unbalance vibration is no longer present in the control signal u. Thus, we need to identify Unb. Actually, an unbalance control algorithm called ABS (Active Balancing System) exists [5], but for stability reasons, it can operate only when the rotational speed is about 20% over the frequency of the rigid mode (about 100 Hz for most machines).

We apply the method called AVR and described in [1]. Its general structure is composed of synchronous sine and cosine generators, low-pass filters and a matrix M representing a rotation of angle θ, which is the main parameter of the compensation method. The role of the synchronous

sine and cosine generators and the low-pass filters is to extract the synchronous part of the measured signal α.

The low-pass filter cut the harmonics further to this operation. The input of the compensation algorithm is the measurement α, and its output is the compensation signal we subtract ξ. We use a high gain for the low-pass filters because the attenuation of the synchronous signal due to unbalance is all the more important since this gain is high. For the output signal, after the rotational matrix M, the sine and cosine generators are used to recompose the signal. It had been shown by a study of stability that the angle θ of the rotational matrix M has to be chosen through the transfer function:

$$\frac{Unb(j\omega)}{\alpha(j\omega)} = \frac{1}{1+G(j\omega)K(j\omega)} = S(j\omega) \tag{13}$$

More precisely, the angle θ is determined thanks to the phase curve of the sensibility function (see figure 3). The complete description of the tuning of θ is available in [1]. A middle range value is used for the application because the compensation has to be shared as well as possible between the two limits of the phase area on which we want to eliminate the unbalance:

$$\theta = \frac{\varphi_1 + \varphi_2}{2} \tag{14}$$

This leads to a value of $\theta = 85°$. Even if the ideal compensation is reached only for the middle point, the system remains stable and convergent on a large zone.

Considering the phase of the compensated system $|\varphi - \theta| = \varphi_c$, the theoretical limit of stability is reached for $\varphi_c = 90°$. In fact, the more we get close to this limit, the more we are likely to destabilize the system. For application purposes, the simulations have shown that stability is preserved with good transitory behaviour if:

$$\begin{cases} |\varphi_1 - \theta| \le \varphi_{\lim} = 70° \\ |\varphi_2 - \theta| \le \varphi_{\lim} = 70° \end{cases} \tag{15}$$

That was confirmed by practical results. We need such a margin to cope with modeling errors or structural defaults. The results we obtain with AVR is shown on figure 5. It shows the power spectrum analysis on the first axis with (solid line) and without AVR (dotted line).

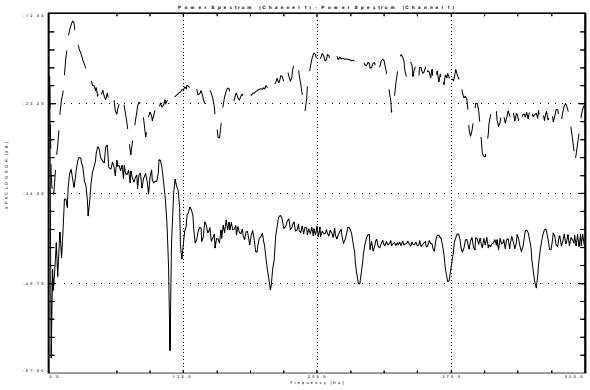

FIGURE 5: Spectrum analysis

This method gives excellent results, but our objective also consists in milling steel. The rotational speed at which we plan to mill is close to the frequency of a mode. Thus, the inconvenience of the AVR algorithm is that it decreases the stiffness of the system for the frequencies around the rotational speed. That's why a new method that preserve the stability of the system had to be designed.

Let Ω be a constant rotational speed. A first signal $\xi = \xi_1$ is added. Then a first measure is made:

$$\alpha_1 = S(j\Omega)(Bal - \xi_1) + \lambda \tag{16}$$

With λ gaussian noise. A second signal ξ_2 is then applied and a new measure α_2 is made:

$$\alpha_2 = S(j\Omega)(Bal - \xi_2) + \lambda \tag{17}$$

In order to choose an unbalance estimator, we need to use the nominal case without noise ($\lambda = 0$). From now on, we just need to resolve the system constituted by the equations (16) and (17). Then, we obtain:

$$\hat{S} = \frac{\alpha_1 - \alpha_2}{\xi_2 - \xi_1} \tag{18}$$

$$\hat{B} = \frac{\alpha_1 \cdot \xi_2 - \alpha_2 \cdot \xi_1}{\alpha_1 - \alpha_2} = \hat{\varepsilon}\, e^{j\hat{\varphi}} \tag{19}$$

We studied the average and the variance of the unbalance estimator (19) in order to find out how ξ_1 and ξ_2 can be chosen to give the best properties possible for the estimator.

We can see on figure 6 the amplitude of the variance of the unbalance estimator versus the phases of the signals added (Parameter 1 and Parameter 2, in degrees), when the amplitudes of ξ_1 and ξ_2 are fixed and different.

The unbalance vector chosen for the simulation has a phase of 30 degrees. We observe on figure 6 that the variance of the estimator increases when the phases of the signals added ξ_1 and ξ_2 get closer. On the other hand, we see that when the two phases are close from each other and close from the phase of the unbalance, the estimator has a variance of almost 0.

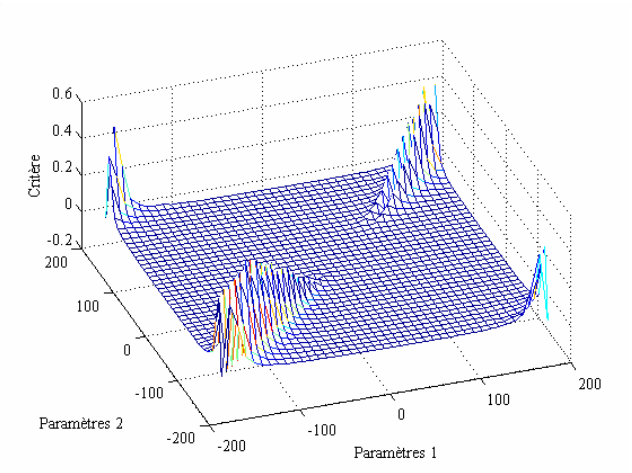

FIGURE 6: Variance of the unbalance estimator

The best situation consists in choosing ξ_1 and ξ_2 out of phase, so that the estimator presents the best variance possible.

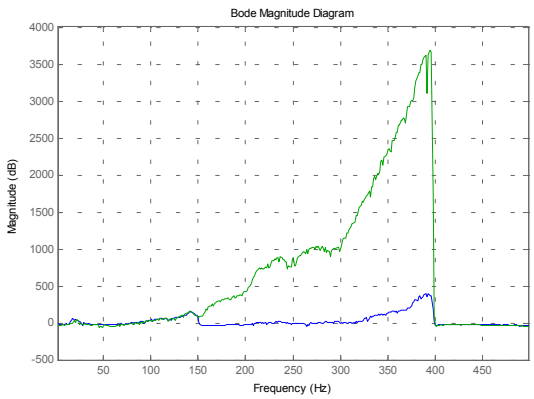

FIGURE 7: Time-domain experiments

We first applied this method to the model obtained before. We then made experiments on the spindle. Figure 7 shows the comparison of two accelerations. The ABS is applied at 400 Hz. The upper curve represents an acceleration without unbalance algorithm, and the lower one shows the result of an acceleration with the last algorithm applied from 150 Hz.

We have now the opportunity to use either ABS, AVR or the last method for unbalance control, depending on the application. The advantage of this last method come from the fact that it is a complete open-loop method, very useful if, as this is the case for milling steel, we need to identify and eliminate the unbalance and at the same time maintain the stability (therefore the stiffness).

CONCLUSION

The objective of this study was to develop a new method for unbalance compensation of a milling spindle on AMBs. This algorithm needs to work for any rotational speed and thus minimize on the whole range of speed the synchronous vibrations due to unbalance.

An accurate model has been developed and used for the tuning of the controller and simulation of the unbalance control algorithm. It has been built in two steps : a modal state-space model for a flexible and gyroscopic rotor combined with a state-space form for the rigid behaviour of the spindle.

The first algorithm applied is AVR. It reduces perfectly the vibrations due to the unbalance, but reduces the stiffness for frequencies around the rotational speed. We then developed an open-loop method with a finite number of measures and signals added. This method needs unbalance to be slightly constant, which is the case here. Both methods have been applied successfully to the spindle.

REFERENCES

[1] Tamisier, Carrère, Font, 2002. *Synchronous unbalance cancellation across critical speed using a closed-loop method.* ISMB8 proceedings, Mito, Japan.

[2] Tamisier, Font, Carrère, 2002. *A new anti-vibration algorithm for active magnetic bearings application*. IEEE Conference on Control Application, Glasgow.

[3] Kim, Lee, 1994. *Isotropic Optimal Control of Active Magnetic Bearing System.* ISMB4 proceedings.

[4] Font, 1995. *Méthodologie pour Prendre en Compte la Robustesse des Systèmes Asservis : Optimisation H∞ et Approche Symbolique de la Forme Standard*. Ph.D. Thesis, Université Paris XI and Supélec.

[5] Matsumura, Kobayashi, 1981. *Fundamental Equations for Horizontal Shaft Magnetic Bearing and its Control System Design*. Electrical Engineering in Japan, Vol. 101, n° 3.